

Green Chemistry

Accepted Manuscript



This is an *Accepted Manuscript*, which has been through the Royal Society of Chemistry peer review process and has been accepted for publication.

Accepted Manuscripts are published online shortly after acceptance, before technical editing, formatting and proof reading. Using this free service, authors can make their results available to the community, in citable form, before we publish the edited article. We will replace this *Accepted Manuscript* with the edited and formatted *Advance Article* as soon as it is available.

You can find more information about *Accepted Manuscripts* in the [Information for Authors](#).

Please note that technical editing may introduce minor changes to the text and/or graphics, which may alter content. The journal's standard [Terms & Conditions](#) and the [Ethical guidelines](#) still apply. In no event shall the Royal Society of Chemistry be held responsible for any errors or omissions in this *Accepted Manuscript* or any consequences arising from the use of any information it contains.



Green Chemistry

PAPER

CO₂ Activation and Fixation: Highly Efficient Syntheses of Hydroxy Carbamates over Au/Fe₂O₃

Received 00th January 20xx,
Accepted 00th January 20xx

DOI: 10.1039/x0xx00000x

www.rsc.org/

Jianpeng Shang,^{*a} Xiaoguang Guo,^b Zuopeng Li,^a and Youquan Deng^c

This paper reports an effective route for the syntheses of hydroxy carbamates from the reaction of CO₂, epoxides and amines catalyzed by Au/Fe₂O₃ catalyst. Under the optimized reaction conditions, various hydroxy carbamates were successfully synthesized with 92–98% isolated yields. The catalyst could be reused for several runs without deactivation. A plausible reaction mechanism was proposed that the hydroxy carbamate was formed through ammonium carbamate intermediate and the catalyst mainly promoted the further nucleophilic addition between epoxide and ammonium carbamate.

1. Introduction

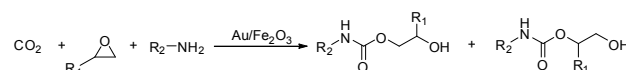
The reduction, capture, or utilization of CO₂ discharge from industrial processes is one of the greatest scientific and technological challenges of the 21st century. Moreover, CO₂ is a nontoxic, abundant and economical C1 feed stock and transformation of CO₂ to other valuable chemicals has attracted significant interests.^{1–13} Among them, catalytic hydrogenation of CO₂ to produce alternate fuels, such as HCOOH, CH₃OH, CH₄, etc, has been extensively studied.^{9–13} However, this technique is severely restricted by the current hydrogen supply. In this regard, the direct usage of CO₂ as building block, *i.e.* carbonyl source, in chemical industry should be an ideal choice.¹ Until now, urea production should be the only way for large scale chemical fixation of CO₂.^{14–15} Thus, there have been increasing interests in developing new routes for direct use CO₂ as carbonyl source.

Hydroxy carbamate and their derivatives are important industrial intermediates for pharmaceutical, organic synthesis, coatings and so on.^{16–18} Generally, the hydroxy carbamates are mainly synthesized by the reaction of cyclic carbonates and amines over organic metal salts such as organic tin, zinc and lead,^{19–20} however, the intrinsic problems that the use of poisonous tin or lead salts and the difficult recycle of catalyst limit their practical applications. Recently, the organocatalyst, such as thiourea and TBD, were reported as efficient metal-free catalyst for the reaction of cyclic carbonates and amines.^{21–23} Moreover, the reaction of CO₂, epoxides and amines could

be a good choice for the development of an environmentally benign method for hydroxyl carbamates synthesis.^{24–26} In the previous reports, the amine substrates are mainly focused on secondary aliphatic amines and the corresponding carbamates isolated yields are relative low. Additionally, such reactions are mainly catalyzed by metal complex homogenous catalysts. Thus, it would be highly desirable to explore an efficient heterogenous catalyst for the reaction of CO₂, epoxide and primary aliphatic or aromatic amines.

Since the discovery that highly dispersed Au nanoparticles supported on metal oxides could be highly active catalysts for CO oxidation,²⁷ Au nanocatalysts have aroused increasing interest in the chemistry community and various Au nanocatalysts have been developed for different chemical reactions including oxidation and hydrogenation, and have shown great promise in catalysis.^{28–31} In particular, the supported Au nanoparticles have also been successfully applied in chemical conversion of CO₂.^{32–33} The unique nature of Au nanoparticles may render the Au nanocatalysts to find more applications in CO₂ conversion.

As far as we know, there was no report for the reaction of CO₂, epoxides and amines (or the reaction of cyclic carbonates and amines, or the reaction of CO₂ and epoxides) catalyzed by Au/Fe₂O₃. Herein, we report the first work to use Au/Fe₂O₃ as highly effective and recoverable catalyst for hydroxyl carbamates syntheses from the reaction of CO₂, epoxides and amines, Scheme 1. Such a process could fulfill the optimum utilization of CO₂, which is of significance from a standpoint of green chemistry and sustainable development.



Scheme 1 The hydroxy carbamates syntheses from CO₂, epoxides and amines over Au/Fe₂O₃

^a Department of Chemistry and Environmental Engineering, Shanxi Datong University, Datong, 037009, China. E-mail: nmsjp2006@126.com; Tel: +86 352 7624721

^b State Key Laboratory of Catalysis, Dalian Institute of Chemical Physics, Chinese Academy of Sciences, Dalian, 116023, China

^c Centre for Green Chemistry and Catalysis, Lanzhou Institute of Chemical Physics, Chinese Academy of Sciences, Lanzhou, 730000, China.

† Jianpeng Shang and Xiaoguang Guo are co-first authors.

2. Experimental

2.1 Hydroxy carbamates synthesis from CO₂, epoxides and amines

All the reactions were conducted in a 90 mL stainless steel autoclave with a glass tube inside equipped with magnetic stirring. In each reaction, CO₂ (1.0-2.0 MPa), epoxide (20-40 mmol), amine (10 mmol) and catalysts (20 mg) were charged successively into the autoclave. After being flushed with CO₂, it was heated up to 80-120 °C and reacted for 8 h. Then, the autoclave was cooled to room temperature and opened to air. The catalyst was separated by centrifugation and filtration. The products were qualitatively and quantitatively analyzed with GC-MS (Agilent 6890/5973), GC (Agilent 7890) equipped with a FID detector and ¹H NMR (Bruker AMX FT 400-MHz)

2.2 Catalysts preparation and characterization

A series of Au/Fe₂O₃ catalysts with different Au loadings (0.8-7.9 wt%) were prepared by co-precipitation method using Fe(NO₃)₃·9H₂O and HAuCl₄·4H₂O as starting materials and Na₂CO₃ as precipitant. Dilute aqueous solutions of 0.62-4.25 mL HAuCl₄·4H₂O (0.1 g mL⁻¹) and 30 mL Fe(NO₃)₃·9H₂O (26 mmol) were mixed uniformly, then added drop-wise into 150 mL aqueous Na₂CO₃ solution (0.47 mol L⁻¹) with vigorous stirring at room temperature, and the pH of the finally resulted solution was controlled to 7-8. After 1 h stirring and 1 h aging, the resulted precipitate was centrifugated (10000 rpm for 15 min), and washed with 2L distilled water under ultrasonic condition. Then, the precursors were calcined at 300 °C for 5 h in air. The calcined catalysts were denoted as n wt% Au/Fe₂O₃, and the n was the Au loadings. The catalysts Fe₂O₃, Cu/Fe₂O₃, Co/Fe₂O₃, Pd/Fe₂O₃, Pt/Fe₂O₃ and Ru/Fe₂O₃ were prepared with the same procedures.

The BET surface areas, pore volumes and average pore diameters of catalysts were obtained with physisorption of N₂ using a Micromeritics ASAP 2010.

High-resolution transmission electron microscope (HR-TEM) analysis was carried out on a JEM 2010 equipped with an energy dispersive X-ray spectrometer (EDXS) and operating at 200 KeV. The catalysts were suspended in ethanol with an ultrasonic dispersion for 10-15 min and then the resulted solution was dropped on a carbon film of copper grid.

X-ray photoelectron spectroscopy (XPS) analysis were measured using a K-Alpha-surface analysis instrument with Al K α radiation (1361 eV) and all the binding energies were referenced to the adventitious C 1s at 285 eV.

X-ray diffraction (XRD) measurements were carried out on a Siemens D/max-RB powder X-ray diffractometer. Diffraction patterns were recorded with Cu K α radiation (40 mA, 40 kV) over the 2 θ range 10-80°.

Temperature-programmed reduction (TPR) of H₂ was carried out on TPR/TPD flow system equipped with an MS detector (DM300, AMETEK, USA). TPR analysis was conducted with 10% H₂/Ar (50 mL min⁻¹). In a typical experiment, the solid sample (120 mg with particle size 160-200 μ m) was pretreated at 300 °C for 1 h under airflow (50 mL min⁻¹) and cooled to room temperature under argon gas flow (50 mL min⁻¹). The profile was recorded at a heating rate of 10 °C min⁻¹ from room

temperature to 300-700 °C and maintained at this temperature until the MS signal of H₂ returned to the baseline.

Temperature-programmed desorption (TPD) of CO₂ and NH₃ was carried out on a TPD flow system equipped with an MS detector (DM300, AMETEK, USA). In a typical experiment, the solid sample (100 mg with particle size 160-200 μ m) was pretreated at 300 °C for 1 h under nitrogen flow (50 mL min⁻¹) and then cooled to room temperature. The sample was subsequently exposed to CO₂ (NH₃) stream (50 mL min⁻¹) at room temperature for 1 h and flushed again with nitrogen for 1 h to remove any physico-adsorbed CO₂ (NH₃). The desorption profile was recorded at a heating rate of 10 °C min⁻¹ from room temperature to 300 °C and maintained at this temperature until the MS signal of CO₂ (NH₃) returned to the baseline.

3. Results and discussions

3.1 Hydroxy carbamates syntheses from CO₂, epoxides and amines

A series of catalysts were screened for the Hydroxy isopropyl phenylcarbamates (HPC) synthesis from CO₂, propylene oxide and aniline, Table 1. In the blank test or in the presence of pure Fe₂O₃ (entry 1-2), the conversion of aniline is trace amount, suggested that the efficient catalyst was essential for such a reaction proceeding successfully. A series of M/Fe₂O₃ (M = Cu, Co, Pd, Pt and Ru) catalysts was further tested and showed poor to moderate catalytic activity for such process and 22-52% aniline conversions were achieved, entries 3-7. For the Au/Fe₂O₃, the aniline conversions were greatly improved when the Au component was introduced and increased with increasing the Au loadings, entries 8-10. For example, 98% of aniline conversion and 99% of HPC selectivity could be achieved over 4.9wt% Au/Fe₂O₃.

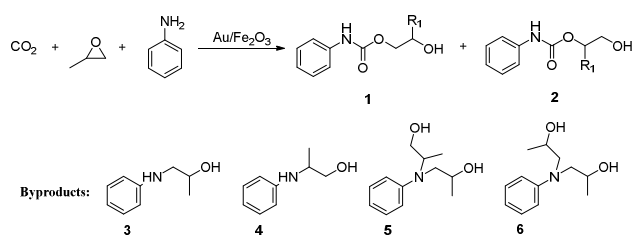
For the target product HPC, the major one defined as **1** by GC-MS corresponds to the nucleophilic ring opening of the propylene oxide at the less substitute site and was preferentially formed with high selectivity in all cases listed in Table 1.³⁴ Meanwhile, the product **2** was also observed, which was formed due to the nucleophilic ring opening of the propylene oxide at methyl substitute site. Additionally, the main byproducts were defined as amino alcohol (such as **3**, **4**, **5** and **6**) by GC-MS, which derived from the ring-opened reaction of epoxides and amines.

Subsequently, the reaction conditions were optimized using 4.9wt% Au/Fe₂O₃ as catalyst. As is easily seen, the conversion of aniline was increased with increasing the reaction temperature and reached 98% at 100 °C (entries 9, 11-12), however, with further increasing the reaction temperature up to 120 °C resulted in a decrease of the HPC selectivity (entry 13). Additionally, both the aniline conversion and HPC selectivity were increased with increasing CO₂ pressure up to 2 MPa (entries 9, 14-15), but those were more sensitive to pressure up to 1.5 MPa, and the effect of pressure on the conversion and selectivity was much smaller at the higher pressure. This could be due to the fact that CO₂ is a reactant and the concentration and solubility of CO₂ in the reaction phase increased with increasing CO₂ pressure. When the

pressure is higher than 1.5 MPa, the concentration of CO₂ in the reaction phase is high enough, and therefore, the effect of pressure on the conversion and selectivity is very limited at the higher pressure.

Moreover, the catalyst was recycled through centrifugation and filtration, and washed with methanol and dried at 100 °C to remove the adsorbed organic materials. The catalyst recycling test showed that the aniline conversion of 96% was obtained even after five runs (entry 16), suggested that the catalyst could be reused without significantly loss in activity after the fifth runs.

Table 1. Hydroxy isopropyl phenylcarbamates (HPC) synthesis under varied catalysts and reaction conditions^a



Entry	Catalyst	T (°C)	CO ₂ pressure (MPa)	Aniline Con. /%	HPC Sel. /% (1:2) ^b
1	--	100	1.5	--	--
2	Fe ₂ O ₃	100	1.5	<1	--
3	4.9wt%Cu/Fe ₂ O ₃	100	1.5	25	68 (93:7)
4	5.0wt%Co/Fe ₂ O ₃	100	1.5	27	94 (95:5)
5	5.1wt%Pd/Fe ₂ O ₃	100	1.5	22	99 (94:6)
6	5.0wt%Pt/Fe ₂ O ₃	100	1.5	43	88 (94:6)
7	5.1wt%Ru/Fe ₂ O ₃	100	1.5	52	98 (95:5)
8	2.8wt%Au/Fe ₂ O ₃	100	1.5	48	96 (95:5)
9	4.9wt%Au/Fe ₂ O ₃	100	1.5	98	99 (95:5)
10	7.9wt%Au/Fe ₂ O ₃	100	1.5	97	99 (95:5)
11	4.9wt%Au/Fe ₂ O ₃	80	1.5	78	98 (94:6)
12	4.9wt%Au/Fe ₂ O ₃	90	1.5	89	99 (95:5)
13	4.9wt%Au/Fe ₂ O ₃	120	1.5	99	95 (95:5)
14	4.9wt%Au/Fe ₂ O ₃	100	1	85	92 (94:6)
15	4.9wt%Au/Fe ₂ O ₃	100	2	99	99 (95:5)
16 ^c	Used 4.9wt%Au/Fe ₂ O ₃	100	1.5	96	99 (95:5)

^a Reaction conditions: 10 mmol aniline; 20 mmol propylene oxide; 20 mg catalyst; 1.0-2.0 MPa CO₂; 80-100 °C; 8 h. Conversions and selectivities were determined by gas chromatography.

^b Numbers in the bracket is the molar ratio of product 1 and 2, and were determined by ¹H NMR.

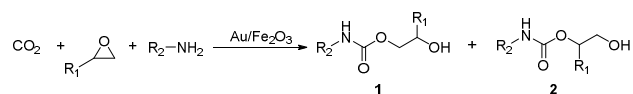
^c Catalyst reused for five times.

In order to investigate the limitation and scope of the catalysts, reactions of CO₂ with various epoxides and amines for corresponding hydroxy carbamates were further carried out over 4.9wt% Au/Fe₂O₃, the results shown in Table 2.

Firstly, the impact of variation of the epoxides on the reaction to form the corresponding hydroxy carbamates was tested, entries 1-5. Excellent yields of the corresponding hydroxy carbamates were obtained with terminal epoxides (entries 1-4), while the disubstituted epoxide, cyclohexene

oxide (entry 5), gave lower activity towards the production of the corresponding hydroxy carbamate, which might be due to the high hindrance of cyclohexene oxide. However, the selectivity of the HPC 1 for the styrene oxide (entry 4) was much lower than that of other epoxides, which might be ascribed to the conjugative effect derived from the benzene ring, which should favourably attack at the carbon atom at which phenyl substitute was connected to afford HPC 2.³⁵

Table 2. Scope and limitation of Au/Fe₂O₃ for catalytic syntheses various hydroxy carbamates^a



Entry	Epoxide	Amine	T (°C)	HPC Yield/% (1:2) ^b
1			100	97
2			100	97 (94:6)
3			100	96 (62:38)
4			100	96 (28:72)
5			100	38
6			100	96 (90:10)
7			100	96 (90:10)
8			100	95 (88:12)
9			100	92 (88:12)
10			80	98
11			80	94
12			80	96
13			80	98
14 ^c			100	96
15 ^c			100	95
16 ^c			100	94
17 ^c			100	96

^a Reaction conditions: 10 mmol amine; 20-40 mmol epoxide; 20 mg 4.9wt% Au/Fe₂O₃; 1.5 MPa CO₂; 80-100 °C; 8 h.

^b Isolated based on the charged amines. Numbers in the bracket is the molar ratio of product 1 and 2, and were determined by ¹H NMR.

^c molar ratio of propylene oxide and diamines = 4.

Then various monoamines with different structures were further investigated, entries 6-13. The results showed that the

yields (92-98%) of the corresponding hydroxyl carbamates were achieved both for aliphatic amines and aromatic amines, however, the reaction temperature for the aliphatic amines were lower than the aromatic amines, suggested that the reaction of CO₂ and propylene oxide with aliphatic amines was easier than aromatic amines, which could be ascribed to the nucleophilicity difference in the two types of amines.

Finally, the hydroxyl dicarbamates were also successfully synthesized in excellent yields (90-96%) from the reaction of CO₂, propylene oxide and diamines, such as 1, 6 - hexamethylenediamine, isophorondiamine, 4, 4 - methylenedicyclohexanamine and 4, 4' - methylenedianiline, entries 14-17. In one word, the reaction of CO₂, epoxides and amines catalyzed by Au/Fe₂O₃ catalyst could be an efficient process for the syntheses of various hydroxy carbamates.

3.2 Results of catalysts characterization

The physical properties of the Au/Fe₂O₃ catalysts are summarized in Table 3. Clearly, the BET surface area of the Au/Fe₂O₃ gradually decreased when the Au component was introduced into the Fe₂O₃, and continuously decreased with increasing of the Au loadings to 2.8wt%, entries 1-3. However, with further increased the Au loadings, the BET surface area of 4.9wt% Au/Fe₂O₃ sharply increased to 163.6 m²/g, and then changed slightly for 7.9wt% Au/Fe₂O₃ (entries 4-5). The variation of the BET surface area of those Au/Fe₂O₃ catalysts combined with their catalytic activities for the hydroxy carbamates syntheses from CO₂, propylene oxide and aniline suggested that the higher BET surface area of the catalysts might be more favourable for the CO₂ absorption and activation.

Table 3. Physicochemical properties of the catalysts

Entry	Catalyst	S _{BET} (m ² /g)	dp ^a (nm)	V _p ^b (cm ³ /g)	Total basic Sites (μmol/g)
1	Fe ₂ O ₃	135.2	11.0	0.40	49
2	0.8wt%Au/Fe ₂ O ₃	131.6	12	0.38	44
3	2.8wt%Au/Fe ₂ O ₃	126.5	12.2	0.35	36
4	4.9wt%Au/Fe ₂ O ₃	163.6	12.4	0.51	29
5	7.9wt%Au/Fe ₂ O ₃	162.7	12.6	0.53	26

^a average pore size

^b average pore volume

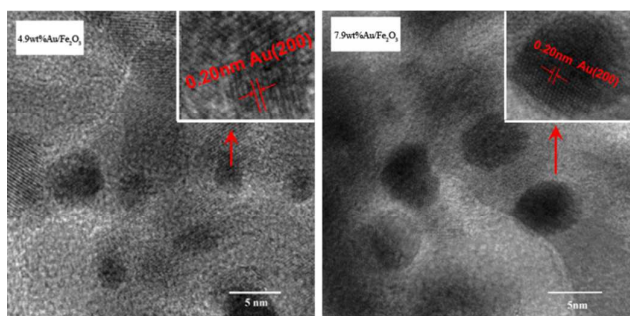


Fig. 1. HR-TEM images of 4.9wt% and 7.9wt% Au/Fe₂O₃, and local lattice of Au (200) plane.

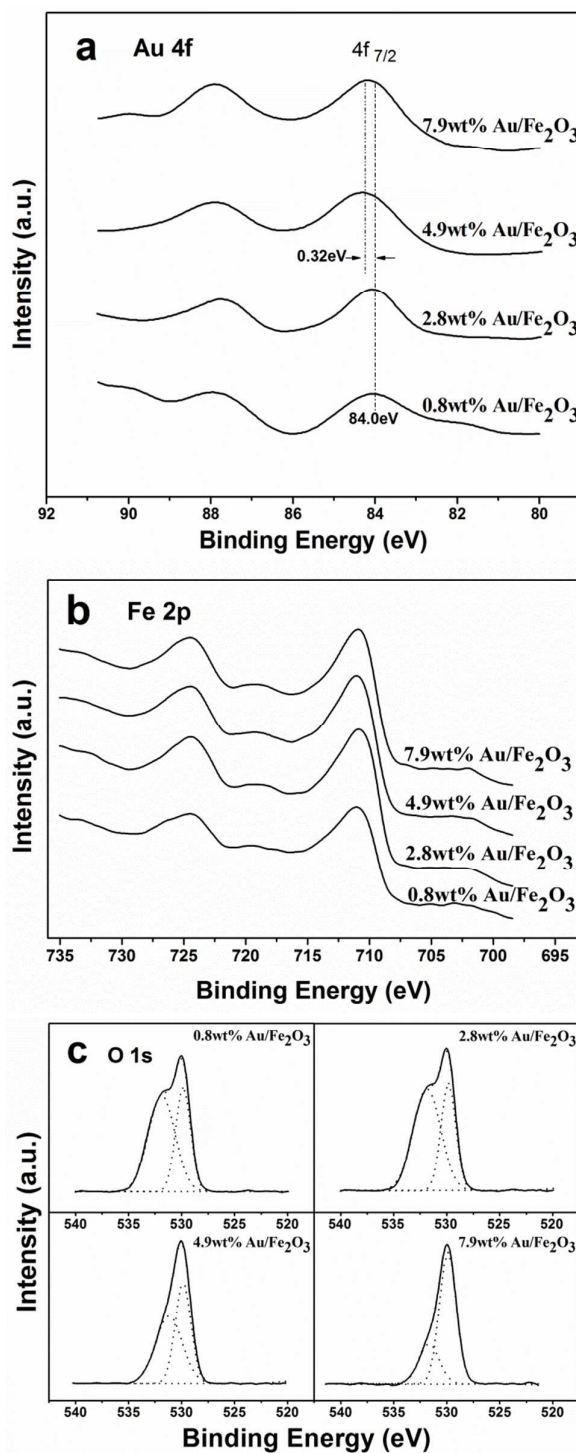


Fig. 2. XPS spectra of (a) Au 4f, (b) Fe 2p and (c) O 1s spectra of Au/Fe₂O₃ with different Au loadings.

The HR-TEM images of the Au/Fe₂O₃ are shown in Fig. 1. From the TEM images, it can be seen that the average size of Au nanoparticles was 3-5nm and the average particle sizes of the Au nanoparticles for 7.9wt% Au/Fe₂O₃ were larger than that for 4.9wt% Au/Fe₂O₃, indicated that the Au nanoparticles

were agglomerated with increasing the Au loadings. Moreover, the Au nanoparticles were spherical and the Au (200) plane was observed in HR-TEM images.

The XPS spectra of Au/Fe₂O₃ with different Au loadings showed that the binding energies of Au 4f_{7/2} and Fe 2p_{3/2} were in the range of 84.0 and 710.7 eV, respectively, suggested that chemical states of Au and Fe species on the catalyst surface were mainly Au⁰ and Fe³⁺, Fig. 2 a and b. Moreover, a positive shift of 0.32eV for the binding energies of Au 4f_{7/2} was observed when the Au loadings reached to 4.9 wt% or higher, indicated that some extent of partially oxidized state Au^{δ+} species could be existed, which might be attributed to the interaction between the Au nanoparticles and the Fe₂O₃ support.³⁶⁻³⁷ As shown in Fig. 1c, two O 1s peaks could be well resolved with their binding energy at 529.8 and 531.7 eV, which should be assigned to oxygen of oxide and hydroxyl groups, respectively.³⁸ Meanwhile, the relative ratio of oxygen of hydroxyl and oxide groups decreased gradually with increasing of Au loadings, suggested that the Au component was favorable for the transformation of Fe(OH)₃ to Fe₂O₃. Furthermore, the surface atom ratio of Au/Fe over 4.9 wt % Au/Fe₂O₃ was 0.011, which was much lower than that of the corresponding bulk composition (0.073), suggested that the Au species might be encapsulated with Fe₂O₃ and acted as a metal substrate to support Fe₂O₃, which leads to an increase of the BET surface area of 4.9wt% Au/Fe₂O₃.

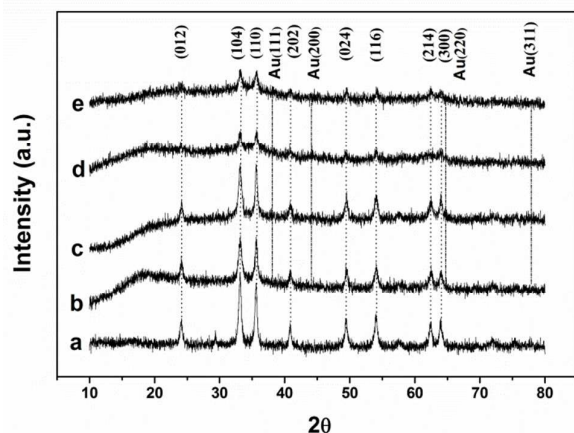


Fig. 3. XRD patterns of (a) Fe₂O₃, (b) 0.8wt% Au/Fe₂O₃, (c) 2.8wt% Au/Fe₂O₃, (d) 4.9wt% Au/Fe₂O₃ and (e) 7.9wt% Au/Fe₂O₃.

XRD patterns of pure Fe₂O₃ and Au/Fe₂O₃ catalysts with different Au loadings are shown in Fig. 3. The results showed that the characteristic diffraction peaks of Fe₂O₃ ($2\theta=33.2^\circ$, 35.7° , 54.1°) were observed for all samples and confirmed Fe₂O₃ formation. For 0.9–4.9wt% Au/Fe₂O₃ samples, the XRD results indicated that the Au species were highly dispersed on the Fe₂O₃ as the characteristic diffraction peaks of Au ($2\theta = 38.2^\circ$, 44.4° , 77.5°) cannot be discerned (Fig.3 b, c and d), however, the characteristic diffraction peaks of Au species were weakly exhibited for 7.9wt% Au/Fe₂O₃ (Fig.2 e), suggested that Au nanoparticles might be agglomerated with higher Au loadings, which is consistent with the results of HR-

TEM. Moreover, the intensity of the Fe₂O₃ diffraction peaks were decreased with increasing of the Au loadings, especially for 4.9wt% and 7.9wt% Au/Fe₂O₃, probably due to the strong interaction of Au nanoparticles and Fe₂O₃.

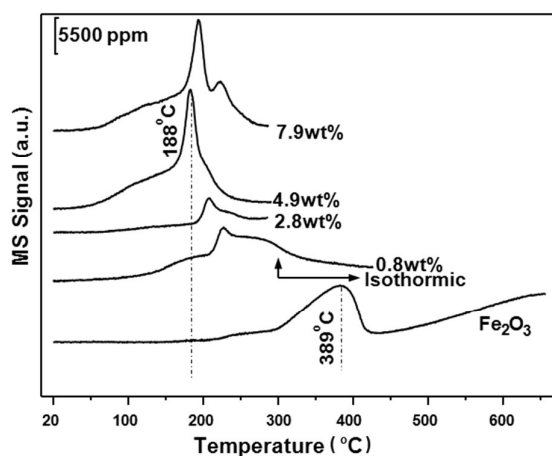


Fig. 4. TPR-H₂ profiles of (a) Fe₂O₃, (b) 0.8wt% Au/Fe₂O₃, (c) 2.8wt% Au/Fe₂O₃, (d) 4.9wt% Au/Fe₂O₃ and (e) 7.9wt% Au/Fe₂O₃.

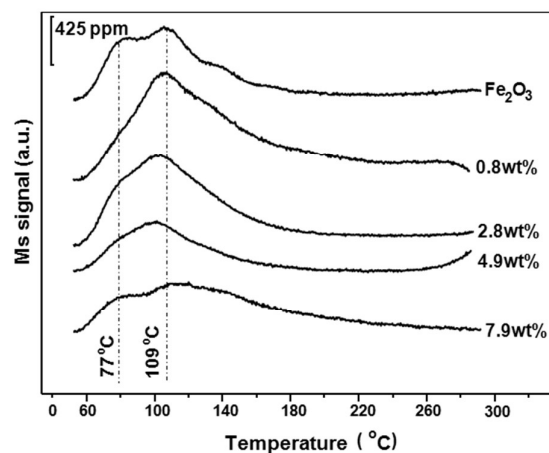


Fig. 5. TPD-CO₂ profiles of (a) Fe₂O₃, (b) 0.8 wt% Au/Fe₂O₃, (c) 2.8 wt% Au/Fe₂O₃, (d) 4.9 wt% Au/Fe₂O₃ and (e) 7.9 wt% Au/Fe₂O₃.

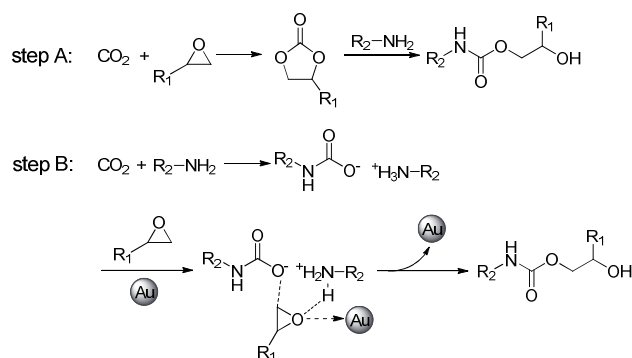
TPR-H₂ results of Fe₂O₃ and Au/Fe₂O₃ with different Au loadings are shown in Fig. 4. For Fe₂O₃, the reduction peak centered at 389 °C was observed, which could be assigned to the reduction of Fe₂O₃ to Fe₃O₄.³⁹ For Au/Fe₂O₃, the reduction peak of Fe₂O₃ to Fe₃O₄ sharply decreased when the Au component was introduced into the Fe₂O₃, and continuously decreased to 188 °C when the Au loadings reached to 4.9wt%. However, the reduction peak of Fe₂O₃ to Fe₃O₄ slightly increased when the Au loadings further increased to 7.9wt%, which might be due to the agglomeration of Au nanoparticles resulted in the weakness of the interaction between Au nanoparticles and Fe₂O₃. The shift in the reduction temperature from 389 to 188 °C suggested that there existed a strong interaction between Au species and Fe₂O₃ support and

addition of Au component favoured the reduction of the iron oxide, which is consistent with the results of XPS and XRD.

The TPD-CO₂ profiles of Fe₂O₃ and Au/Fe₂O₃ with different Au loadings are shown in Fig. 5. Generally, broadened CO₂ desorption peaks in the temperature region of 60–160 °C were observed over all the tested samples, which were derived from the weak strength basic sites. From the quantitative results of TPD-CO₂, it can be seen that the total basic sites ranged from 48 to 29 μmol/g for pure Fe₂O₃ and 4.9wt% Au/Fe₂O₃, respectively, when Au component was added and Au content was increased. Though not shown here, similar TPD-NH₃ characterization was also carried out over the Au/Fe₂O₃ catalysts. Almost no NH₃ desorption peak on the TPD-NH₃ curves could be observed. These TPD-CO₂ (or NH₃) results showed that these catalysts have weak or almost no acidities, but possessed weak basicities.

3.3 Possible reaction mechanism

There may be two possible reaction pathways for the formation of hydroxy carbamates from CO₂, epoxides and amines. One is the hydroxy carbamates formed by the reaction of amines with cyclic carbonate, which could be produced from CO₂ and epoxides (Scheme 2, step A) and another is through the formation of ammonium carbamate intermediate and the hydroxy carbamate was obtained through nucleophilic addition between epoxide and ammonium carbamate (Scheme 2, step B).



Scheme 2 Possible reaction mechanism for the hydroxy carbamate syntheses from CO₂, epoxides and amines over Au/Fe₂O₃

Since the cyclic carbonate was not detected in the reaction mixture of amines, epoxides and CO₂, the formation of hydroxy carbamate by the reaction of amines with cyclic carbonate might be excluded. Therefore, the nucleophilic addition reaction between epoxide and ammonium carbamate is considered as reasonable reaction pathway. Moreover, the ammonium carbamate was readily obtained by the reaction of amines and CO₂,^{7, 40} so the catalysts mainly catalyzed the nucleophilic addition process between epoxide and ammonium carbamate.

According to the results of the characterization and catalytic performance of 4.9wt% Au/Fe₂O₃ catalysts, the formed Au nanoparticles, especially the Au^{δ+} species, would induce

activation of the epoxide ring through coordination with the oxygen atom in epoxides, illustrated in scheme 2 step B. Additionally, the relative larger BET surface area and weak basic site favoured the CO₂ absorption and conversion to the ammonium carbamate, which would be easily nucleophilic attacked on the neighbouring activated epoxides to produce the hydroxy carbamates.

Conclusions

In conclusion, an effective route for the syntheses of hydroxy carbamates from the reaction of CO₂, epoxides and amines over Au/Fe₂O₃ catalyst was developed. Under the optimized reaction conditions, several important hydroxy carbamates were successfully synthesized with 92–98% isolated yields. The Au/Fe₂O₃ catalyst could be reused for several runs without deactivation. The characterization results of the catalysts suggested that the formed Au nanoparticles, larger BET surface area and weak basic sites all favoured the CO₂ absorption and epoxide activation, and resulted in the highly catalytic activity of 4.9wt% Au/Fe₂O₃. A plausible reaction mechanism was also proposed that the hydroxy carbamate was formed through ammonium carbamate intermediate and the catalyst mainly promoted the further nucleophilic addition between epoxide and ammonium carbamate.

Acknowledgements

This work has been financially supported with Doctoral Scientific Research Foundation of Shanxi Datong University (2012-B-12), Basic Research Programs of Science and Technology Department of Datong (2015107) and National Natural Science Foundation of China (No: 21473185 and U1532117).

Notes and references

- 1 T. Sakakura, J. C. Choi and H. Yasuda, *Chem. Rev.*, 2007, **107**, 2365.
- 2 A. J. Hunt, E. H. K. Sin, R. Marriott and J. H. Clark, *ChemSusChem*, 2010, **3**, 306.
- 3 K. Huang, C. L. Sun and Z. J. Shi, *Chem. Soc. Rev.*, 2011, **40**, 2435.
- 4 B. X. Hu, C. Guild and S. L. Suib, *J. CO₂ UTIL.*, 2013, **1**, 18.
- 5 R. Zhang, L. Guo, C. Chen, J. Z. Chen, A. J. Chen, X. G. Zhao, X. R. Liu, Y. H. Xiu and Z. S. Hou, *Catal. Sci. Technol.*, 2015, **5**, 2959.
- 6 Y. Liu, W. M. Ren, K. K. He and X. B. Lu, *Nat. Commun.*, 2014, **5**, 2087.
- 7 J. P. Shang, S. M. Liu, X. Y. Ma, L. J. Lu and Y. Q. Deng, *Green Chem.*, 2012, **14**, 2899.
- 8 L. D. Hao, Y. F. Zhao, B. Yu, H. Y. Zhang, H. J. Xu and Z. M. Liu, *Green Chem.*, 2014, **16**, 3039.
- 9 Z. F. Zhang, Y. Xie, W. J. Li, S. Q. Hu, J. L. Song, T. Jiang and B. X. Han, *Angew. Chem. Int. Ed.*, 2008, **47**, 1127.
- 10 Y. Ohnishi, T. Matsunaga, Y. Nakao, H. Sato and S. Sakaki, *J. Am. Chem. Soc.*, 2005, **127**, 4021.
- 11 F. Arena, K. Barbera, G. Italiano, G. Bonura, L. Spadaro and F. Frusteri, *J. Catal.*, 2007, **249**, 185.

- 12 F. Pontzen, W. Liebner, V. Gronemann, M. Rothaemel and B. Ahlers, *Catal. Today*, 2011, **171**, 242.
- 13 S. Wesselbaum, T. Stein, J. Klankermayer and W. Leitner, *Angew. Chem. Int. Ed.*, 2012, **51**, 7499.
- 14 F. Shi, Y. Q. Deng, T. L. SiMa, J. J. Peng, Y. L. Gu and B. T. Qiao, *Angew. Chem., Int. Ed.*, 2003, **42**, 3257.
- 15 R. Nomura, Y. Hasegawa, M. Ishimoto, T. Toyosaki and H. Matsuda, *J. Org. Chem.*, 1992, **57**, 7339.
- 16 I. Vauthey, F. Valot, C. Gozzi, F. Fache and M. Lemaine, *Tetrahedron Lett.*, 2000, **41**, 6347.
- 17 A. J. Wills, Y. K. Ghosh and S. Balasubramanian, *J. Org. Chem.*, 2002, **67**, 6646.
- 18 J. P. Mayer, G. S. Lewis, M. J. Cuetius and J. Zhang, *Tetrahedron Lett.*, 1997, **38**, 8455.
- 19 J. Huybrechts, *US. Pat.*, 6646153, 2003.
- 20 W. J. Blank, *US. Pat.*, 4820830, 1989.
- 21 M. Blain, L. Jean-Gérard, R. Auvergne, D. Benazet, S. Caillol and B. Andrioletti, *Green Chem.*, 2014, **16**, 4286;
- 22 W. S. Guo, J. Gonzalez-Fabra, N. A. G. Bandeira, C. Bo and A. W. Kleij, *Angew. Chem., Int. Ed.*, 2015, **54**, 11686;
- 23 M. elva, M. abris, V. ucchini, A. erosa and M. Noè, *Org. Biomol. Chem.*, 2010, **8**, 5187.
- 24 F. Kojima, T. Aida and S. Inoue, *J. Am. Chem. Soc.*, 1986, **108**, 391.
- 25 N. Saito, K. Hatakeda, S. Ito, T. Asano and T. Toda, *Bull. Chem. Soc. Jpn.*, 1986, **59**, 1629.
- 26 Y. Yoshida and S. Ionue, *Chem. Lett.*, 1978, 139.
- 27 M. Haruta, T. Kobayashi, H. Sano and N. Yamada, *Chem. Lett.*, 1987, 405.
- 28 M. Kapkowski, P. Bartczak, M. Korzec, R. Sitko, J. Szade, K. Balin, J. Lelatko and J. Polanski, *J. Catal.*, 2014, **319**, 110.
- 29 X. J. Liu, J. F. Liu, Y. P. Li, Y. J. Li and X. M. Sun, *Chemcatchem*, 2014, **6**, 2501.
- 30 N. Perret, X. D. Wang, T. Onfroy, C. Calers and M. A. Keane, *J. Catal.*, 2014, **309**, 333.
- 31 R. Y. Zhong, X. H. Yan, Z. K. R. J. Gao, Zhang and B. Q. Xu, *Catal. Sci. Technol.*, 2013, **3**, 3013.
- 32 F. Shi, Q. H. Zhang, Y. B. Ma, Y. D. He and Y. Q. Deng, *J. Am. Chem. Soc.*, 2005, **127**, 4182.
- 33 D. Preti, C. Resta, S. Squarzialupi and G. Fachinetti, *Angew. Chem., Int. Ed.*, 2011, **50**, 12551.
- 34 S. Bonollo, F. Fringuelli, F. Pizzo and L. Vaccaro, *Synlett*, 2007, **17**, 2683.
- 35 S. Bonollo, D. Lanari and L. Vaccaro, *Eur. J. Org. Chem.*, 2011, **14**, 2587.
- 36 J. Huang, W. L. Dai and K. N. Fan, *J. Catal.*, 2009, **266**, 228.
- 37 A. M. Visco, F. Neri, G. Neri, A. Donato, C. Milone and S. Galvagno, *Phys. Chem. Chem. Phys.*, 1999, **1**, 2869.
- 38 J. F. Moulder, W. F. Stickle, P. E. Sobol and K. D. Bomben, *Handbook of X-ray Photoelec-tron Spectroscopy*, Perkin Elmer, Eden Prairie, 1992.
- 39 A. Venugopal and M. S. Scurrrell, *Appl. Catal., A*, 2004, **258**, 241.
- 40 A. Peeters, R. Ameloot and D. E. De Vos, *Green Chem.*, 2013, **15**, 1550.

An effective route for hydroxyl carbamates syntheses from CO₂, epoxides and amines over Au/Fe₂O₃ was developed. Such a process could fulfill the optimum utilization of CO₂, which is of significance from a standpoint of green chemistry and sustainable development.

